The $\alpha_3(\beta Y_{341}W)_3\gamma$ Subcomplex of the F_1-ATPase from the Thermophilic *Bacillus* PS3 Fails to Dissociate ADP When MgATP Is Hydrolyzed at a Single Catalytic Site and Attains Maximal Velocity When Three Catalytic Sites Are Saturated with MgATP†

Chao Dou,‡ P. A. George Fortes,§ and William S. Allison*,‡

Departments of Chemistry and Biochemistry and of Biology, University of California at San Diego, La Jolla, California 92093-0601

Received July 16, 1998; Revised Manuscript Received October 7, 1998

ABSTRACT: The hydrolytic properties of the $\alpha_3\beta_3\gamma$ and mutant $\alpha_3(\beta Y_{341}W)_3\gamma$ subcomplexes of the TF_1-ATPase have been compared. ATPase activity of the mutant is less sensitive to turnover-dependent inhibition by azide, less suppressed by increasing concentrations of Mg^{2+} during assay, and less stimulated by lauryl dimethylamine oxide (LDAO). Therefore, it has much lower propensity than wild-type to entrap inhibitory MgADP in a catalytic site during turnover. The fluorescence of the introduced tryptophans in the $\alpha_3(\beta Y_{341}W)_3\gamma$ subcomplex is completely quenched when catalytic sites are saturated with ATP or ADP with or without Mg^{2+} present. As reported for the $\beta Y_{331}W$ mutant of *Escherichia coli* F_1 (Weber, J., Wilke-Mounts, S., Lee, R. S.-F., Grell, E., Senior, A. E. (1993) *J. Biol. Chem. 268*, 20126−20133), this provides a direct probe of nucleotide binding to catalytic sites. Addition of stoichiometric MgATP to the mutant subcomplex quenched one-third the tryptophan fluorescence which did not recover after 60 min. This was caused by entrapment of MgADP in a single catalytic site. Titration of catalytic sites of the $\alpha_3(\beta Y_{341}W)_3\gamma$ subcomplex with MgADP or MgATP revealed K_d's of < 50 nM, about 0.25 μM and about 35 μM. Titrations were not affected by azide, whereas LDAO lowered the affinities of catalytic sites 2 and 3 for MgADP by 5-fold and 2-fold, respectively. During titration with MgATP, LDAO slightly lowered affinity at ATP concentrations below 30 μM and had no effect at ATP concentrations above 30 μM. Maximal velocity was attained when the third catalytic site was titrated with MgATP in the presence or absence of LDAO. The same K_d's for binding MgATP to the $(\alpha A_{396}C)_3\beta_3(\gamma A_{22}C)$ mutant were observed before and after inactivating it by cross-linking α to γ. This implies that the different affinities of catalytic sites for MgATP do not represent negative cooperativity, but rather represent heterogeneous affinities of catalytic sites dictated by the position of the coiled-coil of the γ subunit within the central cavity of the $(\alpha\beta)_3$ hexamer.

The F_1-ATPases are the peripheral membrane components of the F_oF_1-ATP synthases found in energy-transducing membranes. When removed from the membrane they are soluble complexes comprised of five gene products with the stoichiometry $\alpha_3\beta_3\gamma\delta\epsilon$ which rapidly hydrolyze ATP. Isolated F_1 contains six nucleotide-binding sites, three of which are catalytic and are present mostly on β subunits with side chains also contributed from adjacent α subunits. The other three binding sites are mostly on α subunits with side chains also contributed from adjacent β subunits. Since a functional role of the latter sites has yet to be defined, they are called noncatalytic nucleotide-binding sites (*1*, *2*).

In the crystal structure of MF_1[1] deduced by Abrahams et al. (*3*), the elongated α and β subunits are arranged alternately in an hexameric aggregate, the central cavity of which contains a coiled-coil comprised of the N- and C-termini of the γ subunit. Whereas each noncatalytic site in the crystal structure is liganded with MgAMP−PNP, the catalytic sites are heterogeneously liganded. One catalytic site, designated β_{TP}, is liganded with MgAMP−PNP, another, designated β_{DP}, is liganded with MgADP, and the third catalytic site, designated β_E, is empty. The catalytic sites of β_{TP} and β_{DP} are in closed conformations, whereas the catalytic site of β_E is in an open conformation (*4*).

Considerable evidence suggests that the three catalytic sites of F_1 participate sequentially during ATP hydrolysis (*5*, *6*). It is also clear from the work of Noji et al. (*7*) that sequential firing of catalytic sites during ATP hydrolysis drives counterclockwise rotation of the coiled-coil contributed by the α-helical carboxyl- and amino-termini of the γ subunit within the central cavity of the $\alpha_3\beta_3$ hexamer. However, there is not universal agreement on the number of catalytic sites saturated with MgATP when maximal velocity is attained during ATP hydrolysis. After substituting βTyr_{331} of *Escherichia coli* F_1 with Trp, Weber et al. (*8*, *9*) correlated

* To whom correspondence should be addressed. Phone: (619)534-3057. Fax: (619)822-0079. E-mail: wsa@checfs2.ucsd.edu.

‡ Department of Chemistry and Biochemistry.

§ Department of Biology.

[1] Abbreviations: TF_1 and MF_1, the F_1-ATPases from the thermophilic *Bacillus* PS3 and bovine heart mitochondria, respectively; LDAO, lauryl dimethylamine oxide; CDTA, *trans*-1,2-diaminocyclohexane-*N*,*N*,*N*′,*N*′-tetraacetic acid.

10.1021/bi981717q CCC: $15.00
Published on Web 11/10/1998

the quenching of fluorescence of the introduced tryptophan residues by MgATP with the hydrolytic activity observed. From the results obtained, it was concluded that the maximal velocity of ATP hydrolysis is attained when three catalytic sites are filled. This conclusion has been challenged by Boyer and colleagues (*10, 11*). They suggest that the fluorescence quenching reported by Weber et al. (*8, 9*) might be tainted by the entrapment of inhibitory MgADP in a catalytic site during the turnover conditions employed: heterogeneity of *E. coli* F_1 caused by partial dissociation of the inhibitory ϵ subunit during assays and competition of free ATP with MgATP for catalytic sites. It is their contention, based on kinetic arguments, that the maximal velocity of ATP hydrolysis is attained when only two catalytic sites are saturated.

When F_1-ATPases hydrolyze low concentrations of ATP, they do indeed entrap inhibitory MgADP in a single catalytic site during turnover (*12, 13*). Low concentrations of ATP are hydrolyzed in three kinetic phases (*14*−*17*). An initial burst slows to an intermediate phase, which is followed by acceleration to a final steady-state rate approaching the initial rate. Transition from the burst phase to the intermediate rate is caused by accumulation of inhibitory MgADP in a catalytic site. This apparently occurs when MgPi dissociates from a catalytic site leaving bound ADP, which then associates with Mg^{2+} derived from the medium. Transition from the intermediate phase to the final rate occurs as MgATP slowly binds to noncatalytic sites, which promotes dissociation of inhibitory MgADP from the affected catalytic site. It has also been shown that dissociation of the inhibitory ϵ subunit of *E. coli* F_1 does occur during assay (*18*).

We report here a thorough kinetic analysis of the $\alpha_3(\beta Y_{341}W)_3\gamma$ mutant subcomplex of the TF_1-ATPase and titration of its catalytic sites with adenine nucleotides in the presence of Mg^{2+} by monitoring quenching of fluorescence of the introduced tryptophan residues. We also report similar titrations of the catalytic sites of the $(\alpha A_{396}C)_3(\beta Y_{341}W)_3\gamma A_{22}C$ triple mutant subcomplex before and after cross-linking the α and γ subunits through a disulfide bond.

EXPERIMENTAL PROCEDURES

Materials. Biochemicals used in assays and buffer components were purchased from Sigma. Dithiothreitol, *o*-iodosobenzoic acid, DEAE-Sephacel, and S-300HR Sephacryl resins were also from Sigma. Toyopearl Butyl-650S resin was from TosoHaas. The oligonucleotides used for mutagenesis were purchase from Gibco BRL. The *E. coli* strains and the plasmids used to prepare the wild-type and mutant $\alpha_3\beta_3\gamma$ subcomplexes were described by Matsui and Yoshida (*19*). The purified enzyme subcomplexes were stored as suspensions in 75% ammonium sulfate at 4 °C.

Construction of Plasmids Containing Mutant Genes. Site-directed mutagenesis was accomplished as described by Kunkel et al. (*20*). The $\alpha_3(\beta Y_{341}W)_3\gamma$ and $(\alpha A_{396}C)_3\beta_3(\gamma A_{22}C)$ mutant subcomplexes were prepared as previously described (*21*). Construction of the plasmid borne genes carrying the $(\alpha A_{396}C)_3(\beta Y_{341}W)_3(\gamma A_{22}C)$ triple mutation was performed by removing the β fragment containing the $Y_{341}W$ substitution (Mlu I−Pst I fragment: 1.4 kb) and ligating it into the pKK−$(\alpha A_{396}C)(\gamma A_{22}C)$ gene fragment (Mlu I−Pst I fragment: 7.3 kb) from which the wild-type β gene fragment was removed. The mutation was checked by restriction enzyme mapping and confirmed by DNA sequencing which failed to reveal additional mutations.

Enzyme Assays. Stock solutions of the enzyme subcomplexes were prepared from pelleted samples of the ammonium sulfate suspensions. Endogenous MgADP was removed from catalytic sites by dissolving the pellets in 50 mM Tris-Cl, pH 8.0, containing 1 mM CDTA. After 1 h the solutions were passed through 1 mL centrifuge columns equilibrated with 50 mM Tris-Cl, pH 8.0, containing 0.1 mM EDTA. The cross-linked form of the $(\alpha A_{396}C)_3(\beta Y_{341}W)_3(\gamma A_{22}C)$ subcomplex was prepared by oxidation with *o*-iodosobenzoate as previously described (*21*). Protein concentrations were determined by the method of Bradford (*22*). ATPase activity was determined spectrophotometrically by ATP regeneration coupled to NADH oxidation (*23*).

Fluorescence Measurements. Fluorescence measurements were performed with a Perkin-Elmer Model MPF-4 spectrofluorometer in the ratio mode at 25 °C. After treatment with CDTA, the TF_1 subcomplexes in 50 mM Tris-HCl, pH 8.0, were diluted to 50 or 100 nM in quartz fluorescence cuvettes to a total volume of 2 mL in the same buffer. During measurements, the protein solutions were magnetically stirred in the cuvettes. For titration experiments, the excitation wavelength was 295 nm and the emission wavelength was 353 nm. The excitation and emission wavelength slits were set at 10 nm. Titrations were carried out by diluting equimolar solutions of $MgCl_2$ with ATP or ADP into the cuvettes containing 2 mL of 50 nM subcomplex plus 1 mM $MgCl_2$ in 50 mM Tris-Cl, pH 8.0. Fluorescence intensity was recorded 30 s after addition of the nucleotide-Mg^{2+} mixture when a stable signal was established. The intensity of the fluorescence was corrected for dilution after the addition of nucleotides. Each titration was repeated at least 3 times.

RESULTS

The $\alpha_3(\beta Y_{341}W)_3\gamma$ Subcomplex of TF_1 has Lower Propensity than Wild-Type to Entrap Inhibitory MgADP in a Catalytic Site during Turnover. An earlier study showed that the $(\alpha D_{261}N)_3\beta_3\gamma$ subcomplex of TF_1 containing defective noncatalytic sites has considerably greater propensity than wild-type to entrap inhibitory MgADP in a catalytic site during ATP hydrolysis (*16*). In contrast, the $\alpha_3(\beta T_{165}S)_3\gamma$ subcomplex entraps little, if any, inhibitory MgADP during turnover (*17, 24*). In another study, it was reported that the V_{max} of the $\alpha_3(\beta Y_{341}W)_3\gamma$ mutant subcomplex is 27 μmol of ATP hydrolyzed mg^{-1} min^{-1} (*21*). This value is 50% greater than that of the wild-type subcomplex, which is 18 μmol of ATP hydrolyzed mg^{-1} min^{-1}, but is considerably less than V_{max} of the $\alpha_3(\beta T_{165}S)_3\gamma$ subcomplex which is 80 μmol of ATP hydrolyzed mg^{-1} min^{-1}. The higher hydrolytic rate of the $\alpha_3(\beta Y_{341}W)_3\gamma$ mutant subcomplex over that of the wild-type subcomplex might reflect a lower propensity to entrap inhibitory MgADP in a catalytic site during ATP hydrolysis. Comparison of hydrolysis of 2 mM ATP by 2 μg of the wild-type $\alpha_3\beta_3\gamma$ and mutant $\alpha_3(\beta Y_{345}W)_3\gamma$ subcomplexes under various conditions shown in Figure 1 supports this contention. Figure 1A illustrates inhibition of hydrolysis of 2 mM ATP by the wild-type $\alpha_3\beta_3\gamma$ subcomplex induced by 2 mM NaN_3 before (traces b, c) and

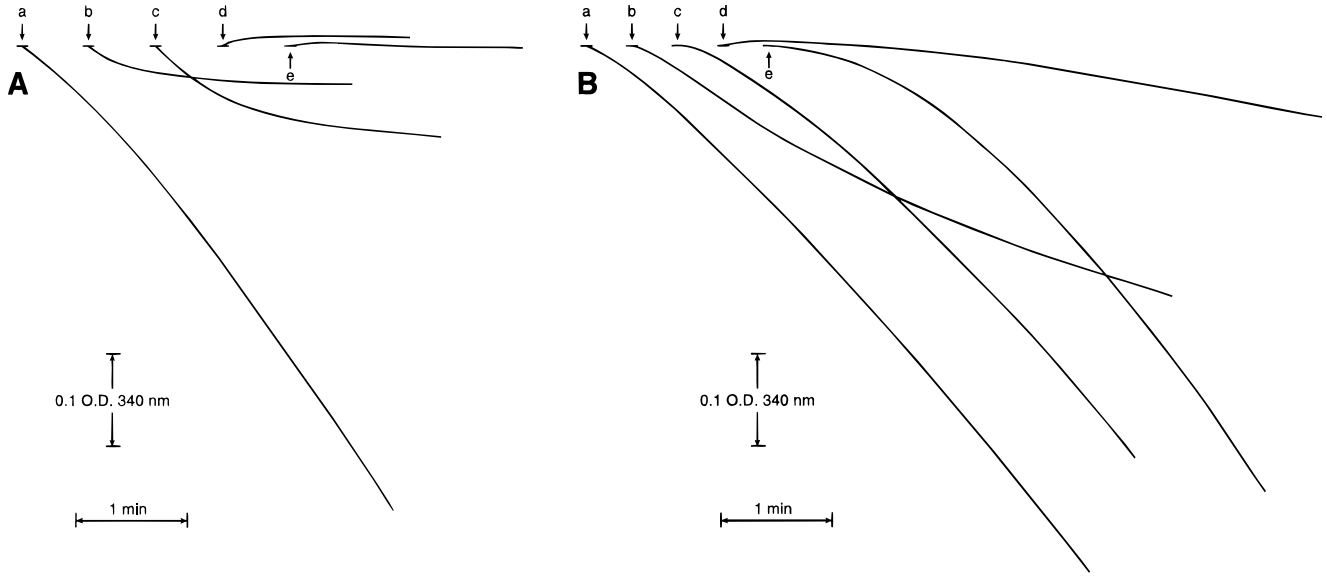

FIGURE 1: Comparison of the effects of azide on hydrolysis of 2 mM ATP by the wild-type $\alpha_3\beta_3\gamma$ and mutant $\alpha_3(\beta Y_{341}W)_3\gamma$ complexes with and without prior binding of MgADP to a single catalytic site in the presence or absence of 0.06% LDAO. Stock solutions, 1 mg/mL, of the wild-type or mutant subcomplex treated with CDTA in 50 mM Tris-HCl, pH 8.0, were prepared as described under Experimental Procedures. (A) Samples, 2 μL each, of stock solutions of the wild-type subcomplex were assayed in medium containing 3 mM Mg^{2+} and 2 mM ATP before (traces a, b, and c) or after (traces d and e) incubation of the subcomplex with a 1.4 molar excess of ADP in the presence of 1 mM $MgCl_2$ for 30 min. Traces b, c, d, and e were obtained with assay medium containing 2 mM NaN_3. Traces c and e were obtained with the same assay medium also containing 0.06% LDAO. Traces are denoted as follows: trace a, control; trace b, plus 2 mM N_3^-; trace c, plus 2 mM N_3^- and 0.06% LDAO; trace d, plus stoichiometric MgADP and 2 mM N_3^-; and trace e, plus stoichiometric MgADP, 2 mM N_3^-, and 0.06% LDAO. (B) Samples, 2 μL each, of stock solutions of the mutant $\alpha_3(\beta Y_{341}W)_3\gamma$ complex were assayed in medium containing 3 mM Mg^{2+} and 2 mM ATP under the various conditions described under A for the wild-type subcomplex.

after (traces d, e) loading a single catalytic site with MgADP, in the absence (traces b, d) or presence (traces c, e) of 0.06% LDAO in the assay medium. In the absence of both effectors (trace a), the wild-type subcomplex hydrolyzes 2 mM ATP with a pronounced initial lag followed by acceleration to a final rate of 18 μmol of ATP hydrolyzed mg^{-1} min^{-1}. When 2 mM azide is present in the assay medium (trace b), ATP hydrolysis decelerates rapidly to a final rate of approximately 0.1 μmol of ATP hydrolyzed mg^{-1} min^{-1}. With 0.06% LDAO in the assay medium, the rate of deceleration induced by azide decreases (trace c). Under these conditions, the final rate is about 0.4 μmol of ATP hydrolyzed mg^{-1} min^{-1}. With LDAO present, maximal inhibition induced by 2 mM azide develops within 3 min (trace c) rather than 2 min (trace b) observed in its absence. However, after loading a catalytic site of the wild-type complex with MgADP before the assay, including 2 mM azide in the assay medium caused immediate inhibition (trace d). The presence of 0.06% LDAO in the assay medium under these conditions did not overcome rapid, azide-induced inhibition of the wild-type subcomplex containing MgADP in a single catalytic site (trace e).

Figure 1B shows that the ATPase activity of the mutant $\alpha_3(\beta Y_{341}W)_3\gamma$ subcomplex responds differently to azide in the assay medium under the same conditions described in Figure 1A for wild-type. In the absence of effectors (trace a), the mutant subcomplex hydrolyzes 2 mM ATP with a short initial lag that accelerates to final rate of 27 μmol of ATP hydrolyzed mg^{-1} min^{-1}. Although 2 mM azide inhibits ATPase activity of the mutant subcomplex by 66% (trace b), the wild-type subcomplex is inhibited by 99.5% under the same conditions. Trace c illustrates that including 0.06% LDAO in the assay medium nearly overcomes inhibition induced by azide. After incubating the mutant subcomplex with stoichiometric ADP in the presence of 2 mM $MgCl_2$, inhibition induced by azide is greater (trace d) than that observed with the apoenzyme (trace b), but again, to a lesser extent than that observed with the wild-type subcomplex under the same conditions. Moreover, addition of 0.06% LDAO to the assay medium overcomes inhibition of the apoenzyme induced by azide (trace c) and also enzyme containing MgADP preloaded at a single catalytic site (trace e). In the case of the apoenzyme (traces b, c), including 0.06% LDAO in the assay medium accelerated ATPase activity 3-fold in the presence of azide, from 9 (trace b) to 27 (trace c) μmol of ATP hydrolyzed min^{-1} mg^{-1}. After loading a single catalytic site of the mutant subcomplex with MgADP, LDAO promoted acceleration of ATP hydrolysis in the presence of azide in the assay medium over that observed in the absence of the detergent by about 34-fold from 0.8 (trace d) to 27 μmol mg^{-1} min^{-1} (trace e).

The decreased sensitivity of the $\alpha_3(Y_{341})_3\gamma$ subcomplex to inhibition by increasing concentrations of Mg^{2+} in the assay medium compared to the wild-type subcomplex also suggests that the mutant enzyme has significantly decreased propensity to entrap inhibitory MgADP in a catalytic site during turnover. For instance, the rate of hydolysis of 2 mM ATP by the wild-type subcomplex is suppressed by 72% when the Mg^{2+} concentration is increased from 2 to 10 mM. In contrast, the ATPase activity of the mutant subcomplex is suppressed by 42% under the same conditions of comparison.

Fluorescence Properties of the Mutant $\alpha_3(\beta Y_{341}W)_3\gamma$ Subcomplex. In the crystal structure of MF_1, βTyr_{345} interacts with the adenine moiety of nucleotides bound to catalytic sites (*3*). Weber et al. (*8*) established that substituting the equivalent residue in the *E. coli* F_1-ATPase with tryptophan

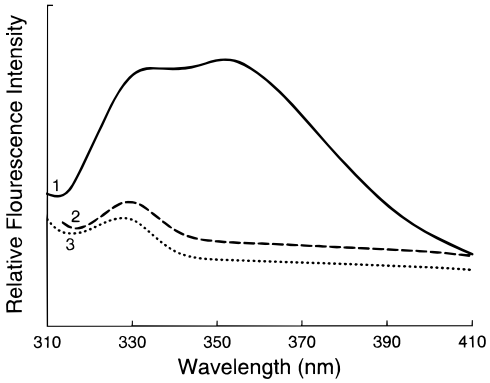

FIGURE 2: The effects of nucleotides on the fluorescence emission spectra of the wild-type $\alpha_3\beta_3\gamma$ and mutant $\alpha_3(\beta Y_{341}W)_3\gamma$ subcomplexes. The subcomplexes were treated with CDTA as described under Experimental Procedures and diluted to 100 nM with 50 mM Tris-HCl, pH 8.0. Curve 1 is the $\alpha_3(\beta Y_{341}W)_3\gamma$ subcomplex in the absence of nucleotides. Curve 2 is the $\alpha_3(\beta Y_{341}W)_3\gamma$ subcomplex in the presence of 1 mM ATP or ADP with or without 1 mM $MgCl_2$ in each case. Curve 3 is the wild-type $\alpha_3\beta_3\gamma$ subcomplex, with or without 1 mM ATP or 1 mM ADP and in the presence or absence of 1 mM $MgCl_2$ in each case.

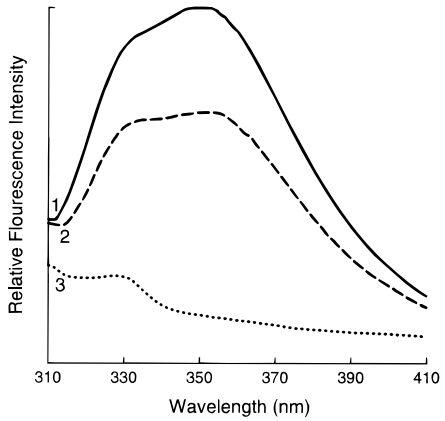

FIGURE 3: Quenching of the fluorescence of the $\alpha_3(\beta Y_{341}W)_3\gamma$ subcomplex by stoichiomtric ATP in the presence of 1 mM Mg^{2+}. The α_3 $(\beta Y_{341}W)_3\gamma$ subcomplex was treated with CDTA as described under Experimental Procedures and diluted to 50 nM with 50 mM Tris-HCl, pH 8.0, before adding stoichiometric ATP and 1 mM $MgCl_2$. Curve 1 is the emission spectrum of the subcomplex in the absence of nucleotides. Curve 2 represents the superimposable traces obtained 1, 10, 20, and 60 min after addition of stoichiometric ATP plus 1 mM $MgCl_2$ to the mutant subcomplex. Curve 3 is the fluorescence emission spectrum of the wild-type subcomplex which is included for reference.

provides a direct probe of binding nucleotides to catalytic sites. This is also the case when tyrosine at position β_{341} of the $\alpha_3\beta_3\gamma$ subcomplex of TF_1 is substituted with tryptophan. The wild-type $\alpha_3\beta_3\gamma$ subcomplex of TF_1-ATPase contains three intrinsic tryptophan residues at position αW_{463} which are located in an α-helix in the C-terminal α-helical domain of the α subunit (*25*). Figure 2 compares the fluorescence emission spectra of the wild-type and the mutant $\alpha_3(\beta Y_{341}W)_3\gamma$ subcomplexes. The wild-type complex (trace 3) fluoresced weakly in the range of 320−420 nm when excited at 295 nm. However, the mutant $\alpha_3(\beta Y_{345}W)_3\gamma$ subcomplex fluoresced substantially (trace 1) when excited at 295 nm with maximal emission occurring at 353 nm. The peaks in the vicinity of 330 nm observed in the emission spectra of the wild-type and mutant subcomplexes reflect Raman scattering by solvent water. Buffer alone exhibited the same Raman scattering pattern. Trace 2 of Figure 2 illustrates that the fluorescence emission spectrum of the mutant $\alpha_3(\beta Y_{341}W)_3\gamma$ subcomplex in the presence of 1 mM ATP plus 1 mM Mg^{2+} decreased to nearly that exhibited by the wild-type enzyme subcomplex. Spectra superimposable with trace 2 were generated when 1 mM ATP or 1 mM ADP in the absence of Mg^{2+} or in the presence of 1 mM Mg^{2+} was added to the mutant subcomplex. No quenching of fluorescence was observed when 1 mM ADP or ATP in the presence of 1 mM Mg^{2+} was added to the 50 nM mutant subcomplex dissolved in 6 M guanidine−HCl. Therefore, the quenching observed in the titrations with the native enzyme reflects binding to specific sites.

Figure 3 shows that the emission spectrum of the $\alpha_3(\beta Y_{345}W)_3\gamma$ subcomplex (trace 1) decreased by about one-third when stoichiometric ATP was added to it in the presence of 1 mM $MgCl_2$ (trace 2). For reference, trace 3 shows the emission spectrum of the wild-type subcomplex. Spectra superimposable with trace 2 were generated 1, 10, 20, and 60 min after the addition of stoichiometric ATP plus 1 mM Mg^{2+}. Since these are the conditions of unisite catalysis (*1*), it was surprising to find that the fluorescence intensity of the reaction mixture did not increase after 60 min. The same results were obtained in the presence of 0.06% LDAO. This suggests that the $\alpha_3(\beta Y_{341}W)_3\gamma$ subcomplex releases product ADP extremely slowly during unisite catalysis. That this is indeed the case was demonstrated by comparing hydrolysis of 2 mM ATP by the wild-type and mutant subcomplexes 60 min after stoichiometric ATP or ADP was added to them in the presence of 1 mM Mg^{2+} with controls not containing nucleotides during prior incubation. Figure 4A compares the rate of hydrolysis of 2 mM ATP by the untreated $\alpha_3(\beta Y_{341}W)_3\gamma$ mutant subcomplex (trace a) and by the mutant subcomplex after prior incubation for 60 min with stoichiometric ADP (trace b) or stoichiometric ATP (trace c). Trace d illustrates hydrolysis of 2 mM ATP in the presence of 1 mM NaN_3 after prior incubation of the mutant subcomplex with stoichiometric ATP for 60 min. The immediate, nearly complete inhibition observed in the presence of azide indicates that a single catalytic site of the mutant subcomplex is occupied with MgADP 60 min after adding stoichiometric ATP to it in the presence of 1 mM Mg^{2+}. Figure 4B illustrates that the wild-type subcomplex behaves identically when submitted to the same conditions. Therefore, the $\beta Y_{341}W$ substitution is not responsible for the slow dissociation of MgADP from the single catalytic site of the mutant subcomplex.

The Effects of Azide and LDAO on Quenching of Fluorescence of the $\alpha_3(\beta Y_{341}W)_3\gamma$ *Subcomplex by MgATP and MgADP*. Figure 5 illustrates the titration of catalytic sites of the $\alpha_3(\beta Y_{341}W)_3\gamma$ subcomplex with MgATP and MgADP assessed by fluorescence quenching of the introduced tryptophan residues in the presence and absence of 1 mM NaN_3 or 0.06% LDAO. During titrations with nucleotides, the fluorescence emission signal at 353 nm stabilized within 30 s after addition of MgATP or MgADP to 50 nM enzyme in 50 mM Tris-Cl, pH 8.0. To ensure that all added ATP and ADP remained as the Mg^{2+} chelate, 1 mM $MgCl_2$ was also present in the buffer. The occupancy of catalytic sites was determined, and curve fitting was performed by the methods described by Weber et al. (*8*). It is clear from Figure 5 that 1 mM azide (■) has no effect on the titration of catalytic

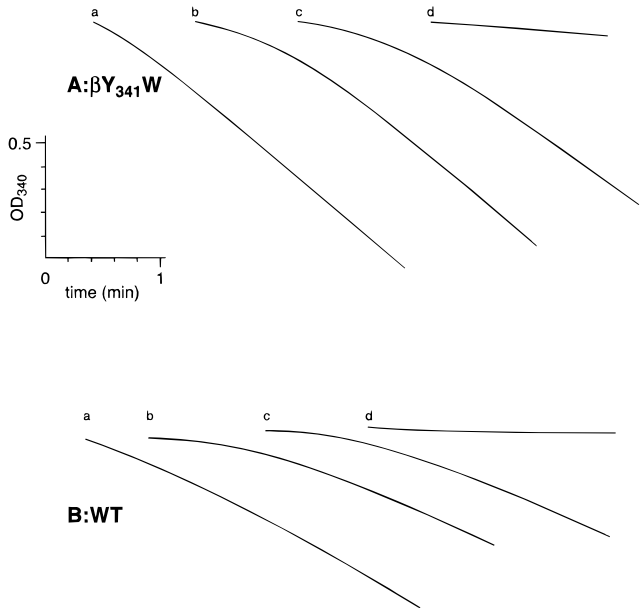

FIGURE 4: The effect of incubation of the wild-type and α_3-$(\beta Y_{341}W)_3\gamma$ subcomplex with stoichiometric ATP for 60 min on ATPase activity in the presence and absence of azide. (A) To 100 μL of 1 mg mL^{-1} $\alpha_3(\beta Y_{341}W)_3\gamma$ subcomplex in 50 mM Tris-HCl, pH 8.0, containing 1 mM $MgCl_2$ was added a, nothing; b, stoichiometric ADP; and c and d, stoichiometric ATP. The mixtures were incubated at room temperature for 60 min at which time 3 μL samples were assayed with 2 mM ATP and a regeneration system in the absence (traces a, b, and c) or presence (trace d) of 1 mM NaN_3. (B) The wild-type subcomplex was treated identically except that 2 μL samples were assayed.

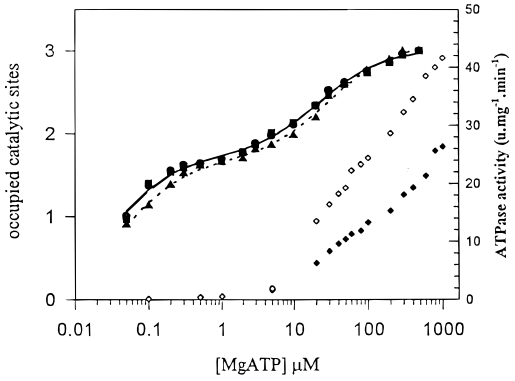

FIGURE 5: Correlation of fluorescence titrations of catalytic sites of the $\alpha_3(\beta Y_{341}W)_3\gamma$ subcomplex with MgATP with and without azide or LDAO with rates of ATP hydrolysis. The α_3 $(\beta Y_{341}W)_3\gamma$ subcomplex was treated with CDTA as described under Experimental Procedures. Solutions for fluorescence measurements were prepared in cuvettes by adding a concentrated solution containing equal concentrations of ATP and $MgCl_2$ to 2 mL of 50 nM subcomplex in 50 mM Tris-Cl containing 1 mM $MgCl_2$, pH 8.0, with no additions (●), plus 1 mM NaN_3 (■), or plus 0.06% LDAO (▲). Relative fluorescence intensity was recorded 30 s after addition of MgATP. ATPase activity was measured at the concentrations of ATP indicated using 2 μL samples of a 1 mg mL^{-1} solution of the α_3 $(\beta Y_{341}W)_3\gamma$ subcomplex with (◇) and without (◆) 0.06% LDAO added.

sites with MgATP, whereas 0.06% LDAO (▲) shifts the titration curve at low MgATP concentrations to the right without affecting the titration curve above 30 μM MgATP. Figure 5 also illustrates the specific activity of the mutant subcomplex when assayed over the concentration range of 0.1−1000 μM ATP in the presence (◇) and absence (◆) of 0.06% LDAO. It is clear from correlation of the data points for ATP hydrolysis with the curves for fluorescence quenching that maximal velocity is attained as the third catalytic site is titrated with MgATP in the presence and absence of LDAO.

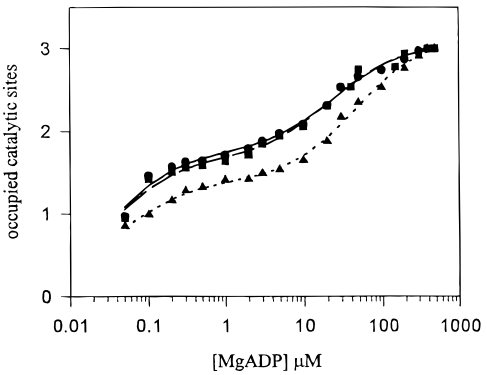

FIGURE 6: Fluorescence titration of catalytic sites of the α_3-$(\beta Y_{341}W)_3\gamma$ subcomplex of TF_1 with MgADP with and without azide or LDAO. The α_3 $(\beta Y_{341}W)_3\gamma$ subcomplex was treated with CDTA as described under Experimental Procedures. Solutions for fluorescence measurements were prepared in cuvettes by adding a concentrated solution containing equal concentrations of ADP and $MgCl_2$ to 2 mL of 50 nM subcomplex in 50 mM Tris-Cl containing 1 mM $MgCl_2$, pH 8.0, with no additions (●), plus 1 mM NaN_3 (■), or plus 0.06% LDAO (▲). Relative fluorescence intensity was recorded 30 s after addition of MgATP.

Table 1: K_d Values for Binding MgATP and MgADP to the Catalytic Sites of the Mutant $\alpha_3(\beta Y_{341}W)_3\gamma$ Subcomplexes of TF_1 under Various Conditions[a]

	$\beta Y_{341}W$			$\alpha A_{396}C/\beta Y_{341}W/\gamma A_{22}C$	
titrant	no. of additions	plus N_3^-	plus LDAO	reduced	oxidized
MgATP					
K_{d2} (μM)	0.25	0.26	0.43	0.30	0.24
K_{d3} (μM)	35	36	42	26	25
MgADP					
K_{d2} (μM)	0.21	0.3	1.2	0.4	0.8
K_{d3} (μM)	34	33	69	27	25

[a] The K_d's for binding MgATP and MgADP were obtained from fits to the three independent binding site models described by Weber et al. (*8*). In all cases, the first catalytic site was filled or nearly completely filled at the lowest nucleotide concentration examined. K_{d1} in each case is estimated to be less than 50 nM.

Figure 6 illustrates titration of catalytic sites with MgADP under the same conditions used for titration with MgATP. Again, 1 mM azide (■) has no effect on the titration curve. However, 0.06% LDAO (▲) shifts the titration curve substantially to the right indicating that it lowers the affinity of catalytic sites of the $\alpha_3(\beta Y_{341}W)_3\gamma$ subcomplex for MgADP.

The K_d values calculated for the titration of the second and third catalytic sites under the various conditions of Figures 5 and 6 are summarized in Table 1. The K_d values calculated for titration of catalytic sites 2 and 3 with MgATP or MgADP in the absence of LDAO or azide are remarkably similar. Whereas 1 mM azide has essentially no effect on these K_d's, 0.06% LDAO decreases the affinities of catalytic site 2 and catalytic site 3 for MgADP by at least 5-fold and about 2-fold, respectively. LDAO shifts the titration curve for MgATP at substrate concentrations below 40 μM to the right, thus lowering the apparent affinities of catalytic sites 2 and 3 by 60% and 20%, respectively.

The Effect of Cross-Linking the α and γ Subunits on Fluorescence Titrations with MgATP and MgADP. It has been shown that cross-linking α to γ or β to γ in the mutant $(\alpha A_{396}C)_3\beta_3(\gamma A_{22}C)$ or mutant $\alpha_3(\beta D_{390}C)_3(\gamma S_{90}C)$ subcomplexes of TF_1, respectively, by oxidation abolishes ATPase activity (*21*). The oxidized subcomplexes are completely reactivated when the introduced disulfide bonds are reduced with dithiothreitol. To determine the effect of immobilizing the γ subunit on binding adenine nucleotides to catalytic sites, the $(\alpha A_{396}C)_3(\beta Y_{341}W)_3(\gamma A_{22}C)$ triple mutant was prepared. The reduced, triple mutant subcomplex has a V_{max} of 23 μmol of ATP hydrolyzed mg^{-1} min^{-1}, which is nearly that of the $\alpha_3(\beta Y_{341}W)_3\gamma$ subcomplex. ATP hydrolysis catalyzed by the single mutant and reduced triple mutant responds similarly to azide and LDAO.

To prepare the cross-linked subcomplex, the triple mutant was treated with *o*-iodosobenzoate (*21*). When ATP hydrolysis catalyzed by the triple mutant was inactivated by greater than 99%, the reaction mixture was passed through two successive centrifuge columns of Sephadex G-50 to remove excess oxidant. Figure 7A shows that the titrations of the oxidized (●) and reduced (■) enzyme subcomplexes with MgATP generate superimposable curves. However, the titration curves of the oxidized and reduced subcomplexes generated with MgADP shown in Figure 7B are not superimposable. The resulting K_d's given in Table 1 indicate that formation of the α−γ cross-link decreases the affinity of catalytic site 2 for MgADP by a factor of 2 without affecting the affinity of catalytic site 3 for MgADP.

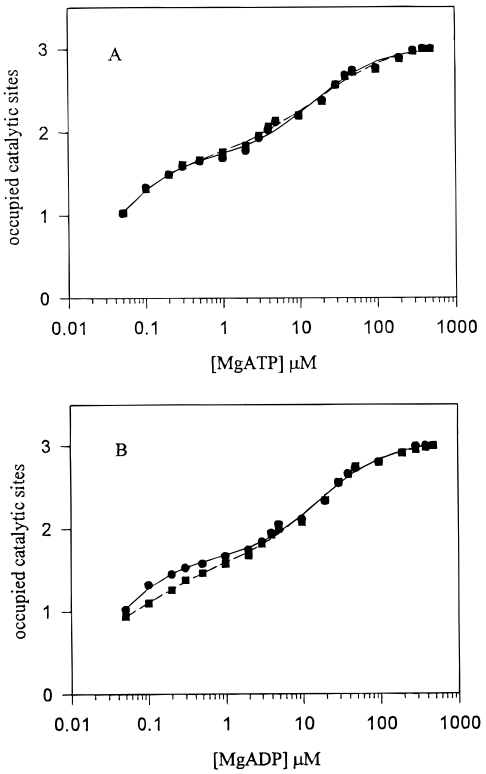

FIGURE 7: Fluorescence titration of catalytic sites of the $(\alpha A_{396}C)_3(\beta Y_{341}W)_3(\gamma A_{22}C)$ subcomplex of TF_1 with MgATP before and after cross-linking α to γ. The α and γ subunits of the $(\alpha A_{396}C)_3(\beta Y_{341}W)_3(\gamma A_{22}C)$ triple mutant were cross-linked by oxidation with *o*-iodosobenzoate as described under Experimental Procedures. The reduced form of the triple mutant was prepared by incubating the CDTA-treated preparation with 2 mM dithiothreitol in 50 mM Tris-HCl, pH 8.0, for 10 min and then passing it through a centrifuge column of Sephadex G-50 equilibrated with 50 mM Tris-HCl, pH 8.0. (A) For titration with MgATP, the cuvettes containing the reduced subcomplex also contained 1 mM dithiothreitol: (●), titration with the oxidized mutant subcomlplex; (■), titration with the reduced mutant subcomplex. (B) For MgADP titration, a concentrated stock solution containing equimolar ADP and $MgCl_2$ was added in increasing amounts to cuvettes containing 2 mL of 50 nM oxidized (●) or reduced (■) mutant subcomplex in 50 mM Tris-Cl containing 1 mM $MgCl_2$, pH 8.0, as described under A.

DISCUSSION

This study was initiated to determine to what extent the $\alpha_3(\beta Y_{341}W)_3\gamma$ subcomplex of TF_1 entraps inhibitory MgADP in a catalytic site during ATP hydrolysis and to what extent the entrapped MgADP contributes to quenching fluorescence of the introduced tryptophans. It is clear from kinetic comparisons that the mutant subcomplex has much lower propensity than wild-type to entrap inhibitory MgADP in a catalytic site during turnover. It is also clear that it has higher propensity for turnover-dependent entrapment of inhibitory MgADP in a catalytic site than the $\alpha_3(\beta T_{165}S)_3\gamma$ subcomplex. Since the latter mutant subcomplex entraps very little, if any, inhibitory MgADP in a catalytic site during turnover (*17*), the $\alpha_3(\beta T_{165}S/Y_{341}W)_3\gamma$ double mutant was prepared and examined by the methods described. Surprisingly, the double mutant has catalytic and nucleotide-binding characteristics nearly identical to those described for the $\alpha_3(\beta Y_{341}W)_3\gamma$ single mutant indicating that the altered catalytic properties introduced by the $\beta Y_{341}W$ substitution override those introduced by the $\beta T_{165}S$ substitution.

Titrations of the tryptophan fluorescence of the $\alpha_3(\beta Y_{341}W)_3\gamma$ subcomplex of TF_1 were modeled according to Weber et al. (*8*) who reported nearly identical results for cooperative binding of MgATP to catalytic sites of the $\beta Y_{331}W$ mutant of *E. coli* F_1. In a recent review, Weber and Senior (*26*) tabulated K_d values of 0.5 and 25 μM for binding MgATP to catalytic sites 2 and 3 of *E. coli* F_1, which correspond closely to the K_d values of 0.25 and 36 μM given in Table 1 for binding MgATP to catalytic sites 2 and 3 of the $\alpha_3(\beta Y_{341}W)_3\gamma$ subcomplex of TF_1. In contrast, the K_d values of 0.20 and 34 μM reported here for binding MgADP to catalytic sites 2 and 3, respectively, of the $\alpha_3(\beta Y_{341}W)_3\gamma$ subcomplex differ considerably from the single K_d value of 20 μM reported for catalytic sites 2 and 3 of the $\beta Y_{331}W$ mutant of *E. coli* F_1. The absence of the δ and ϵ subunits in the TF_1 subcomplex may be responsible for this difference. This premise is supported by the following observations. Immobilization of the γ subunit in the $(\alpha A_{396}C)_3(\beta Y_{341}W)_3(\gamma A_{22}C)$ triple mutant subcomplex of TF_1 via a disulfide bond to the α subunit does not affect affinities of catalytic sites for MgATP or MgADP. In contrast, Grüber and Capaldi (*27*) found that cross-linking of the α subunit in the $(\alpha S_{411}C)_3(\beta Y_{331}W)_3\gamma(\epsilon S_{108}C)$ mutant *E. coli* F_1 to ϵ alone or to ϵ and γ strongly alters the affinities of catalytic sites for MgATP.

The observation that cross-linking of the γ subunit to the α subunit in the $(\alpha A_{396}C)_3(\beta Y_{341}W)_3(\gamma A_{22}C)$ triple mutant has little or no effect on the widely different affinities of the three catalytic sites of the TF_1 subcomplex for MgATP or MgADP is consistent with the observation of Grüber and Capaldi (*27*) that cross-linking of β to γ and ϵ in the $\alpha_3(\beta Y_{331}W)_3\gamma(\epsilon S_{108}C)$ double mutant of *E. coli* F_1 has little

effect on binding MgATP to catalytic sites. These observations suggest that the different affinities for MgADP or MgATP observed in the titrations do not reflect negative cooperativity, but rather reflect heterogeneous affinities of catalytic sites dictated by the position of the asymmetric coiled-coil of the γ subunit within the central cavity of the $(\alpha\beta)_3$ hexamer. The observation that the $\alpha_3\beta_3$ subcomplex of TF_1 does not exhibit apparent negative cooperativity of MgTNP-ATP binding supports this contention (*27*).

In agreement with titration of catalytic sites of the $\beta Y_{331}W$ mutant of *E. coli* F_1 with MgATP reported by Weber et al. (*8*), maximal velocity is not attained until three catalytic sites of the $\alpha_3(\beta Y_{341}W)_3\gamma$ mutant subcomplex of TF_1 are saturated with MgATP in the presence or absence of LDAO. The fluorescence titrations of catalytic sites with MgATP were performed with the mutant $\alpha_3\beta_3\gamma$ subcomplex of TF_1 in the presence of 1 mM excess Mg^{2+} over ATP and were slightly affected by LDAO at low, but not at high, substrate concentrations. Therefore, the contention of Milgrom et al. (*11*) that the fluorescence titrations of catalytic sites of the $\beta Y_{331}W$ mutant of *E. coli* F_1 with MgATP reported by Weber et al. (*8*) might be tainted by enzyme heterogeneity due to dissociation of the ϵ subunit, competition of free ATP with MgATP for catalytic sites, and/or interference from inhibitory MgADP does not apply to the $\alpha_3(\beta Y_{341}W)_3\gamma$ subcomplex of TF_1. Given the close similarity of the fluorescence titrations of catalytic sites of the mutant TF_1 subcomplex and the mutant *E. coli* enzyme with MgATP, the reservations of Milgrom et al. (*11*) are not likely to apply to the $\beta Y_{331}W$ mutant of *E. coli* F_1.

The kinetic analyses reported by Milgrom et al. (*11*) supporting their contention that F_1-ATPases attain maximal velocity when only two catalytic sites are saturated with MgATP deserve comment. By using conventional steady-state kinetic analysis, that is, when the same assay system is employed over the entire range of ATP concentrations examined, several laboratories have reported two K_m's in the micromolar range for ATP hydrolysis by F_1-ATPases corresponding to bisite catalysis (K_m's of 1−4 μM) and trisite catalysis (K_m's of 40−250 μM) (*29*−*31*). Moreover, steady-state kinetic analysis of the $\alpha_3(\beta T_{165}S)_3\gamma$ subcomplex of TF_1 revealed K_m values of 1.4 and 110 μM with associated k_{cat} values of 14 and 340 s^{-1}, respectively (*17*). The kinetic analyses cited above employed ATP regeneration with pyruvate kinase coupled to NADH oxidation by the pyruvate released with lactate dehydrogenase to determine rates over the entire range of ATP concentrations examined. In contrast, Milgrom et al. (11) report a single K_m value of 130 μM with an associated k_{cat} of 700 s^{-1} for nucleotide-depleted MF_1 over the ATP concentration range of 0.1−800 μM. The coupled ATP regeneration system was employed to assay nucleotide-depleted MF_1 activated with pyrophosphate for monitoring hydrolysis of 5−800 μM ATP and release of ^{32}Pi from [γ-^{32}P]ATP for monitoring hydrolysis of 0.1−5 μM ATP with unactivated MF_1 in the absence of an ATP regeneration system. It seems likely that the use of very different assays at high versus low ATP concentrations is responsible for the failure of Milgrom et al. (*11*) to observe a K_m in the 1−5 μM range during ATP hydrolysis catalyzed by nucleotide-depleted MF_1.

The observation that the tryptophan fluorescence of the $\alpha_3(\beta Y_{341}W)_3\gamma$ subcomplex was quenched by one-third on addition of stoichiometric MgATP which did not recover after an hour due to entrapment of MgADP is not consistent with the characteristics of "unisite" catalysis reported for intact TF_1. Yohda and Yoshida (*32*) reported that addition of substoichiometric ATP to TF_1 is accompanied by rapid release of ADP and Pi. The absence of the δ and ϵ subunits in the $\alpha_3\beta_3\gamma$ subcomplex may be responsible for the different characteristics of "unisite" catalysis by TF_1 and the subcomplex. In this regard, it is interesting that Xiao and Penefsky (*33*) reported that hydrolysis of substoichiometric ATP by the five subunit preparation of *E. coli* F_1 is not accelerated appreciably by a chase with 5 mM ATP, whereas the four subunit, δ-less enzyme, exhibits a cold chase typical of ATP hydrolysis at a single catalytic site of MF_1 (*1, 34*).

The failure to observe release of ADP from a single catalytic site 1 h after adding stoichiometric ATP in the presence of Mg^{2+} to the wild-type and mutant subcomplexes is consistent with experiments reported by Drobinskaya et al. (*35*). They observed entrapment of inhibitory MgADP in a single catalytic site of nucleotide-depleted MF_1 after adding stoichiometric ATP to the enzyme in the presence of Mg^{2+}. Consistent with this finding, Chernyak and Cross (*36*) reported that inhibitory Mg(2-N_3-ADP) was entrapped in a single catalytic site of MF_1 after adding stoichiometric 2-N_3-ATP to it in the presence of Mg^{2+} in the dark. Furthermore, it has been demonstrated that considerable [α-^{32}P]ADP fails to release when substoichiometic [α, γ-^{32}P]-ATP is hydrolyzed at a single catalytic site of MF_1 (*37*). In contrast, Milgrom and Cross (*38*) have recently reported that product ADP and Pi dissociate at nearly equal rates (about 5.5×10^{-3} s^{-1}) after adding substoichiometric ATP to nucleotide-depleted MF_1 followed by diluting the enzyme 667-fold in buffer plus 1.1 mg mL^{-1} BSA. Release of products was assessed by passing samples of diluted enzyme through centrifuge columns of Sephadex equilibrated with the same buffer containing 1.1 mg mL^{-1} BSA. In the studies where slow dissociation of ADP was observed, slow release of ADP was assessed by enzyme assay (*35*, *36*), by enzyme assay and quenching of tryptophan fluorescence of the α_3-$(\beta Y_{341}W)_3\gamma$ subcomplex of TF_1, and by passing samples through centrifuge columns in the absence of BSA (*37*). Consideration of these differences suggests that BSA might influence the rate of dissociation of ADP when MgATP is hydrolyzed at a single catalytic site.

REFERENCES

1. Penefsky, H. S., and Cross, R. L. (1991) *Adv. Enzymol. Relat. Areas Mol. Biol. 64*, 173−214.
2. Pedersen, P. L., and Amzel, L. M. (1993) *J. Biol. Chem*, *268*, 9937−9940.
3. Abrahams, J. P., Leslie, A. G. W., Lutter, R., and Walker, J. E. (1994) *Nature 370*, 621−628.
4. Allison, W. S. (1998) *Acc. Chem. Res.* (in press).
5. Boyer, P. (1993) *Biochem. Biophys Acta 1140*, 215−250.
6. Weber, J., and Senior, A. E. (1996) *J. Biol. Chem. 271*, 3474−3477.
7. Noji, H., Yasuda, R., Yoshida, M., and Kinosita, K., Jr. (1997) *Nature 386*, 299−302.
8. Weber, J., Wilke-Mounts, S., Lee, R. S−F., and Senior, A. E. (1993) *J. Biol. Chem. 268*, 20126−20133.
9. Weber, J., Wilke-Mounts, S., and Senior, A. E. (1994) *J. Biol. Chem. 269*, 20462−20467.
10. Boyer, P. D. (1997) *Annu. Rev. Biochem. 66*, 717−749.

11. Milgrom, Y. M., Murataliev, M. B., and Boyer, P. D. (1998) *Biochem. J. 330*, 1037−1043.
12. Vasilyeva, E. A., Minkov, I. B., Fitin, A. F., and Vinogradov, A. D. (1982) *Biochem. J. 202*, 9−14.
13. Vasilyeva, E. A., Minkov, I. B., Fitin, A. F., and Vinogradov, A. D. (1982) *Biochem. J. 202*, 15−23.
14. Jault, J. M., and Allison, W. S. (1993) *J. Biol. Chem. 268*, 1558−1566.
15. Paik, S. R., Jault, J.-M., and Allison, W. S. (1994) *Biochemistry 33*, 126−133.
16. Jault, J. M., Matsui, T., Jault, F. M., Kaibara, C., Muneyuki, E., Yoshida, M., Kagawa, Y., and Allison W. S. (1995) *Biochemistry 34*, 16412−16418.
17. Jault, J.-M., Dou, C., Grodsky, N. B., Matsui, T., Yoshida, M., and Allison, W. S. (1996) *J. Biol. Chem. 271*, 28818−28824.
18. Dunn, S. D., Tozer, R. G., and Zadorozny, V. D. (1990) *Biochemistry 29*, 3225−4340.
19. Matsui, T., and Yoshida, M. (1995) *Biochim. Biophys. Acta 1231*, 139−146.
20. Kunkel, T. A., Benebek, K., and McClary, J. (1991) *Methods Enzymol. 204*, 125−139.
21. Dou, C., Grodsky, N. B., Matsui, T., Yoshida, M., and Allison, W. S. (1997) *Biochemistry 36*, 3719−3727.
22. Bradford, M. M. (1976) *Anal. Biochem. 72*, 248−254.
23. Jault, J.-M., and Allison, W. S. (1994) *J. Biol. Chem. 269*, 319−325.
24. Allison, W. S., Jault, J.-M., Grodsky, N. B., and Dou, N. B. (1995) *Biochem. Soc. Trans. 23*, 752−756.
25. Shirakihara, Y., Leslie, A. G. W., Abrahams, J. P., Walker, J. E., Ueda, T., Sekimoto, Y., Kambara, M., Saika, K., Kagawa, Y., and Yoshida, Y. (1997) *Structure 5*, 825−836.
26. Weber, J., and Senior, A. E. (1997) *Biochim. Biophys. Acta 1319*, 19−58.
27. Grüber, G., and Capaldi, R. A. (1996) *J. Biol. Chem. 271*, 32623−32628.
28. Kaibara, C., Matsui, T., Hisabori, T., and Yoshida, M. (1996) *J. Biol. Chem. 271*, 2433−2438.
29. Gresser, M. J., Myers, J. A., and Boyer, P. D. (1982) *J. Biol. Chem. 257*, 12030−12038.
30. Wong, S.-Y., Matsuno-Yagi, A., and Hatefi, Y. (1984) *Biochemistry 23*, 5004−5009.
31. Roveri, O., and Calcaterra, N. B. (1985) *FEBS Lett. 192*, 123−127.
32. Yohda, M., and Yoshida, M. (1987) *J. Biochem. (Tokyo) 102*, 875−883.
33. Xiao, R., and Penefsky, H. S. (1994) *J. Biol. Chem. 269*, 19232−19237.
34. Grubmeyer, C., Cross, R. L., and Penefsky, H. S. (1982) *J. Biol. Chem. 257*, 12092−12100.
35. Drobinskaya, I. Y., Kozlov, I. A., Murataliev, M. B., and Vulfson, E. N. (1985) *FEBS Lett. 182*, 419−424.
36. Chernyak, B. V., and Cross, R. L. (1992) *Arch. Biochem. Biophys. 295*, 247−252.
37. Bullough, D. A., Verburg, J. G., Yoshida, M., and Allison, W. S. (1987) *J. Biol. Chem. 262*, 11675−11683.
38. Milgrom, Y. M., and Cross, R. L. (1997) *J. Biol. Chem. 272*, 32211−32214.

BI981717Q